Navigable map-aided differential odometry to enhance GNSS in adverse conditions

Clément Fouque, Philippe Bonnifait

Navigable Map-Aided Differential Odometry to Enhance GNSS in adverse conditions

Clément Fouque, Philippe Bonnifait
Heudiasyc UMR 6599, Université de Technologie de Compiègne

***Abstract*—This paper studies the benefits of integrating proprioceptive measurements and a-priory geographical knowledge in the GNSS computation to increase availability and accuracy for modern ITS applications. A tightly-coupled framework for merging GNSS pseudo-ranges and odometric measurements is first introduced. An efficient way to merge a 2D navigable road-map is then presented, including the road selection and the map measurement model. A cautious fusion strategy, which provides enhanced GNSS-like positioning is performed, using an Extended Kalman filter monitoring innovation signals. This method has been applied to real-field data recorded during spring 2007. Results show the benefits of the proposed framework for GPS-computation under adverse conditions, i.e. with bad satellites availability and configuration.**

I. Introduction

In the recent years, many Intelligent Transportation Systems (ITS) and field robotic applications have been developed. Most of these applications are underlaid by a global positioning provider and a geo-referenced database. In this case, the positioning provider estimates the current location of the vehicle. It must fulfill availability, reliability and accuracy requirements coming from the application. To address this problem, many positioning solutions have been studied. Using a GNSS receiver is the easiest way to provide a global location. Unfortunately, a standalone receiver can be subject to signal degradation or outages in adverse conditions. Here, adverse conditions mean bad satellites availability (less than 4 satellites in direct view with a good geometrical configuration) and multipath. To tackle these issues, the GNSS receiver is commonly fused with proprioceptive sensors, such as odometers, wheel speed sensors or inertial measurements [1], [2], [3], [4]. Additionally, GNSS data can be either loosely, or tightly integrated with dead-reckoning (DR). In tight integration, the GNSS pseudo-ranges are directly exploited [5], [6]. It allows taking advantages of the few available measurements in case of averse conditions. This helps to reduce the unavoidable proprioceptive estimation drift which is not possible with a loosely coupled scheme that suffers from complete outages when less than four satellites are visible. This configuration is also more efficient to reject multipath coming from signal propagation troubles [7].

Navigable road-maps are becoming very common and affordable nowadays. Using such an information is a promising issue to correct the location estimates drift in adverse conditions since the road network of the map contains absolute information that can constraint the solution [8], [9], [10], [11]. The road network can be used either as a positioning sensor [12] or as virtual base station to provide DGPS corrections [13]. As a standard navigable map is often subject to offset and since the vehicle rarely drives exactly on the poly-lines, these techniques introduce biases in the estimated location [14]. This issue can be tackled using a precise map describing the road space using multi-poly lines [15], [16].

In this paper, a Kalman-based fusion process merging GNSS measurements and proprioceptive measurements together with a navigable road-map is presented in order to provide a GNSS-like positioning information. The process relies on trustworthy wheel speed sensors (WSS) that provide an estimated motion of the vehicle. These are tightly fused with the raw GNSS pseudo-ranges. Additionally, a method to integrate a standard 2D navigable road-map into the fusion process is presented. We propose to use it as a compass sensor which allows taking into account easily the unavoidable map offset. Since the GNSS pseudo-ranges and the map can introduce both faulty measurements, an internal consistency test is considered to reject outliers. It is based on the monitoring of innovation signals gated thanks to a statistical threshold.

The paper is organized as follows. First, the state-space description of the vehicle is given, including the process model for the state prediction and the sensor models for the state update. The use of a 2D navigable road-map is presented in the second section. The third section details the Kalman-based fusion process. It includes the map-matching strategy for selecting the correct road segment and the consistency test used for faulty measurements rejection. Finally, experimental results are given to illustrate the efficiency of the proposed framework using EGNOS corrections.

II. Problem definition

A. Working frame

In order to merge GNSS measurements with DR measurements, expressed relatively to the vehicle body-frame, the use of a local working frame is convenient to elaborate an evolution model [17, Chap. 10.4]. For that, a East - North - Up (ENU) navigation frame is defined. This frame is tangent to the Earth ellipsoid at a given reference point, close to the working area. This frame is valid only for a limited area and thus, must be updated from time to time. The satellites coordinates, usually given in Earth Centered-Earth Fixed (ECEF) coordinates, have to be transformed.

B. Process model

The process model used for the Kalman predictive step relies on a locally circular linear interpolation of a 2D

differential-drive motion model. It is assumed to be locally planar. According to the tight integration of GNSS measurements, additional parameters must be considered. The vehicle altitude in the local frame is introduced using a constant elevation model. Additionally, the GNSS receiver clock offset is considered using a first-order polynomial model, allowing the offset to evolve during a complete outage. Therefore, the following state vector X_k is :

$$X_k = \left[x, y, z, \psi, v, \omega, d, \dot{d}\right] \tag{1}$$

Where (x, y, ψ) describes the 2D vehicle pose, z its altitude in the local frame, (v, ω) the linear and angular velocities of the vehicle, and $(d, \dot{d})$ the GNSS receiver clock offset and drift. So, a discrete motion model can be given by, T_e being the sampling period:

$$\begin{cases} x_{k+1} &= x_k &+ T_e v_k \cos(\psi_k + \frac{1}{2} T_e \omega_k) \\ y_{k+1} &= y_k &+ T_e v_k \sin(\psi_k + \frac{1}{2} T_e \omega_k) \\ z_{k+1} &= z_k & \\ \psi_{k+1} &= \psi_k &+ T_e \cdot \omega_k \\ v_{k+1} &= v_k & \\ \omega_{k+1} &= \omega_k & \\ d_{k+1} &= d_k &+ T_e \cdot \dot{d}_k \\ \dot{d}_{k+1} &= \dot{d}_k & \end{cases} \tag{2}$$

The vehicle evolution model is then depicted by a set of non-linear equations, where α_k is the process model error:

$$X_{k+1} = f\left(X_k\right) + \alpha_k \tag{3}$$

C. Sensor models

1) Dead-Reckoning: According to the hypothesis made in Section II-B, the rear WSS provide good estimates of the linear speeds of the wheels. With v_l (resp. v_r) denoting the left (resp. right) linear wheel speed, the observation model of the DR sensors is given by the following linear equation set:

$$\begin{bmatrix} v_l \\ v_r \end{bmatrix} = \begin{bmatrix} 1 & -\frac{L}{2} \\ 1 & \frac{L}{2} \end{bmatrix} \cdot \begin{bmatrix} v \\ \omega \end{bmatrix} \tag{4}$$

Where L is the rear axle length.

2) GNSS measurements: To realize the tight integration of the GNSS raw measurements, the L1 pseudo-ranges (PR) are used. Using broad-casted ephemeris and a SBAS[1] such as EGNOS in Europe, the measured PRs can be corrected by taking into account SV (Space Vehicle) clock offset dt and elongation due to atmospheric effects. By denoting R the distance, the PR observation model [17] can be reduced to:

$$\rho = R + d + \beta_\rho \tag{5}$$

With these corrections, PR errors β_ρ are assumed to be zero-mean, Gaussian and uncorrelated . Additionally, the SBAS system provides an estimated PR error variance [18], which is mandatory in a Bayesian fusion framework.

[1]Satellite Based Augmentation System

III. Navigable Road Maps

A. Road Cache

Commonly, a navigable road map is a database that contains a vectored description of the road network. Each road in the database is identified by a unique identification (Id), and is described by both geometrical and topological information. Each road is spatially sampled and described by a set of shape points and two nodes (origin and end). These points form a polygonal curve describing the shape of the road center-line. The number of carriageways and line width are also often known. In addition, a connectivity table is given, allowing the user to known which roads are connected with a given Id. This connectivity table is usually used for path planning. It can also improve the tracking of the roads [19].

A complete navigable road map represents a huge amount of data, even for offline computation. Thus, a reduced road cache is extracted around a given point [19]. This extraction point is set as the reference point of the working frame (Sec.II-A). Indeed, the working frame must be updated each time a new road cache is requested. Before being usable, the shape points and nodes are converted into the working frame. Additionally, several road features, such as segment heading and length, are precomputed to speed up the map-matching process. This is a second advantage of using a road cache.

B. Map usage

Unfortunately, a digital road map is subject to bad precision (i.e. low spatial sampling) and bad accuracy (ie. absolute offset). Therefore, using the road shape for constraining the position estimation induces non zero-mean errors which can affect badly any Bayesian estimation process. Since the precision of the map is often better than its accuracy, we suggest to use the heading information provided by the polygonal curve describing the road, under the hypothesis that the car heading is parallel to the road. The DR process can take advantage of this information, as its drift is very dependent of the quality of the heading estimate [20].

In order to handle unavoidable position offset, the map observation itself is quite simple since it is only a heading information, according to the driving direction. Let us suppose for simplification that the right segment has been map-matched. By denoting ψ_r this segment heading, the observation model used for map update is:

$$\psi_r = \psi_k + \beta_\psi \tag{6}$$

Where β_ψ represents the observation model error.

IV. Cautious fusion strategy

Next, a method for tight integration of GNSS PR with 2D geographic information and DR measurements is introduced. The DR measurements are supposed to be trustworthy (no outlier). This is mandatory since the DR estimates need to be reliable in our fusion strategy. Figure 1 illustrates the fusion process.

First, the current position is predicted according to Eq. 2 and is then updated according to the WSS measurements.

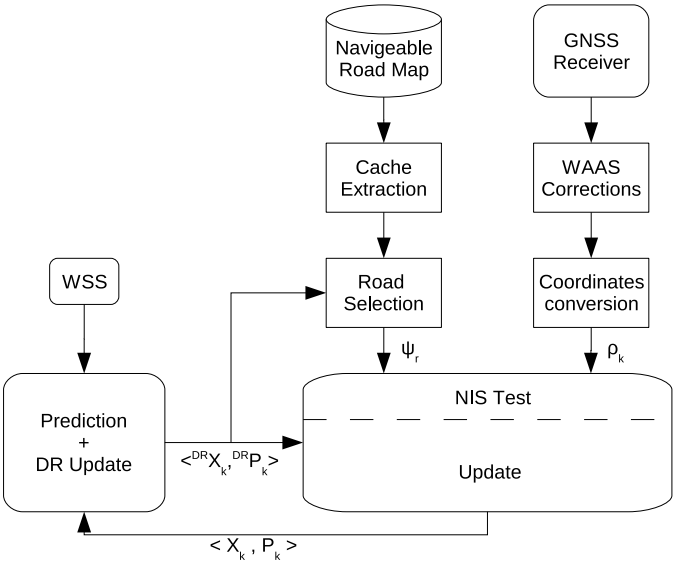

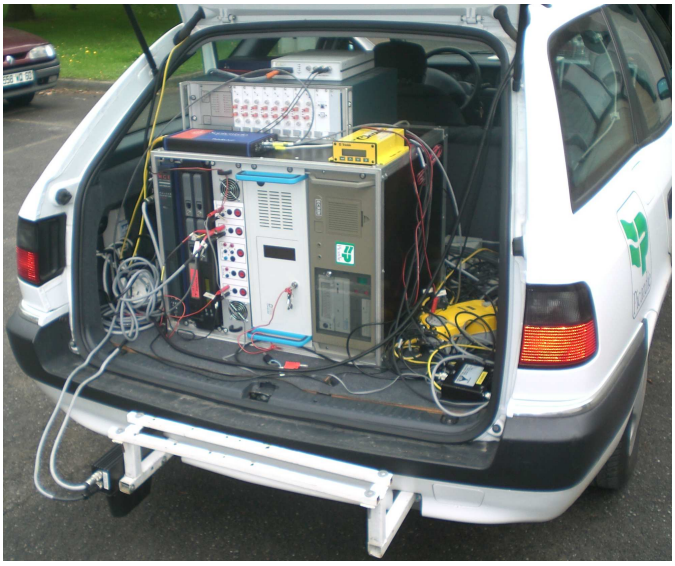

Figure 2. Experimental vehicle.

In the pose tracking process, the road cache is updated if needed and the most-likely road segment is identified in a cautious way according to vehicle pose after the DR update.

Contrary to the DR measurements, the GNSS receiver and the road map can provide faulty measurements. Thus, these measurements are validated through an internal consistency test before being fused. The map observation is validated using the Mahalanobis distance between the DR estimated pose $X_{k|k,DR}$ and the pose computed according to the selected road [12]. It is given by the following expression:

$$\Delta_r = \frac{d^2}{\sigma_d^2 + \lambda_{max}^2} + \frac{\Delta\psi^2}{\sigma_r^2 + \sigma_\psi^2} \tag{7}$$

The GNSS PR are validated using a Normalized Innovation Squared (NIS) test. The NIS value is also computed according to the DR estimated pose $X_{k|k,DR}$. It is given by:

$$\eta_k = \frac{1}{2}\nu_k.Q_\nu^{-1}.\nu_k \tag{8}$$

Where ν is the innovation and Q_ν its covariance matrix. The innovation vector is the difference between the current PRs vector ρ_k and the predicted measurement corresponding to the predicted state $X_{k|k-1,DR}$:

$$\nu_k = \rho_k - h(X_{k|k-1,DR}) \tag{9}$$

Where $h(X_{k|k-1,DR})$ is the non-linear observation model derived from the GNSS observation model.

In case of an Extended Kalman Filter, the innovation covariance matrix is given by:

$$Q_\nu = H_k.P_{k|k-1,DR}.H_k^T + Q_\rho \tag{10}$$

Where H_k is the jacobian matrix of the observation model.

Finally, a threshold value is computed using the χ^2 distribution given a False Alarm probability for each Δ_r and η_k. If Δ_r and η_k are greater than their corresponding threshold, the measurement is not consistent with the noise model with a high probability [21] and is rejected. Otherwise, accepted measurements are fused (Eq 5 and 6) to compute the new estimated state $X_{k|k}$.

V. Experimental results

Experiments have been carried out in May 2007 using an experimental vehicle of the Heudiasyc laboratory (Figure 2). The reference path of the vehicle has been recorded using a Trimble 5700 DGPS PPK receiver and 4 base stations from the French Orpheon network. The car was driven in Compiegne suburbs, which constitute an open area with occasional tree foliage leading to GPS errors and bad geometrical configuration of the SV constellation. For all the following experiments, a unique road cache was used with the reference point located at 49°23´ 6.36”N, 2°47´ 2.04”E.

A. Map-aided differential odometry

The performance of map-aided DR is first compared to un-aided DR. The estimator is first initialized using GNSS and DR measurements. Figure 3 shows the position estimates in the ENU frame for the DR estimations with and without map-aiding. It also shows the reference trajectory and an emphasis is made on locations where the map is used. Figure 4 depicts the angular velocity estimation error for the un-aided DR. This chart shows that differentiating the WSS measurements provides a noisy angular velocity estimates. Thus, the estimated location is degraded. In addition, the RMS error signal for the map-aided DR is provided by Figure 5. The RMS error signal for DR estimates using a fiber-optic yaw-rate gyro (KVH400) is also given.

According to Figure 3, differential odometry alone is not able to provide a correct estimation for a long period of time. If a long outage occurs, the state estimates diverge significantly. Now, considering the estimated trajectory using the map-aided DR, a major improvement can be seen. With the map, the

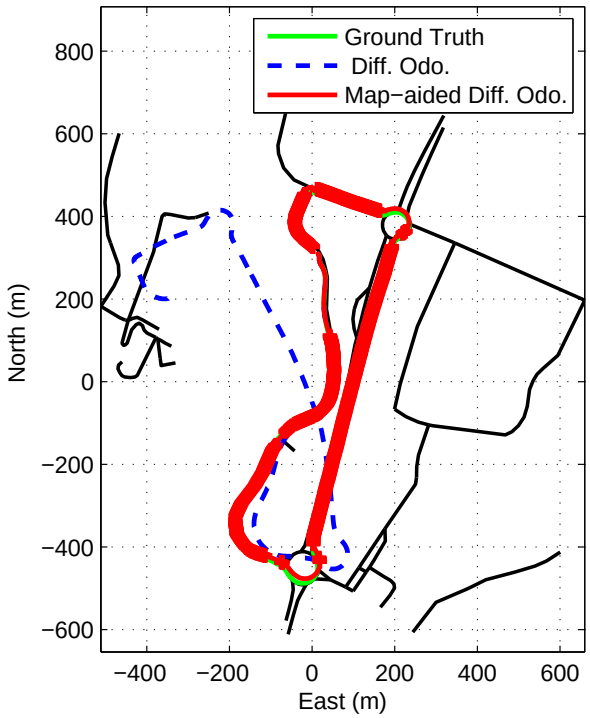

Figure 3. ENU trajectory estimates for un-aided differential odometry and map-aided differential odometry.

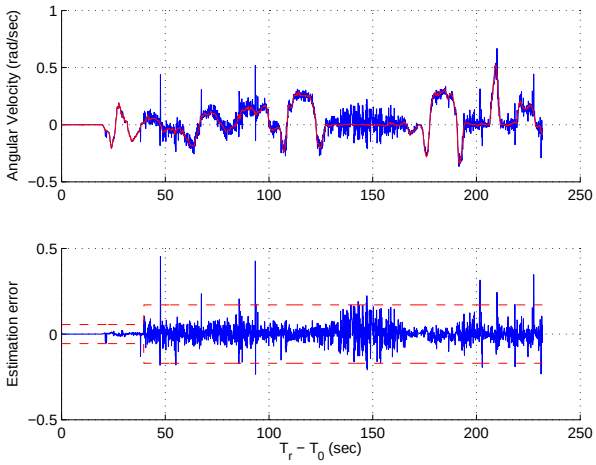

Figure 4. Estimated Angular velocity for the differential odometry compared to the measured angular velocity provided by an optic-fiber gyro.

fusion process is able to keep a correct location estimates in spite of noisy angular velocity estimates. During this trail, the map is used 54% of time, including the initialization process. Now considering the RMS error signal, the map-aided DR shows interesting perfomances in comparison with the DR estimates using a fiber-optic gyro. After a $2km$-long loop, the RMS error of the map-aided DR is about $10m$, to be compared with the $2m$ error for the gyro-aided DR. This is a good result knowing that only the WSS have been used to estimate the rotational speed.

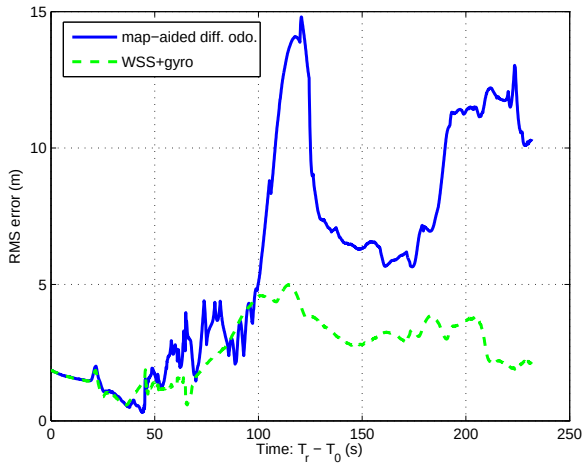

Figure 5. RMS error for map-aided DR compared with the result obtained using the WSS and a fiber optic gyro (KVH400).

B. Adverse GNSS visibility conditions

In this second experiment, adverse GNSS visibility conditions are considered. A simulated urban canyon has been defined around the straight line between the two roundabouts. It has been applied using a sectoral mask on the available SVs. Thus, the GNSS visibility is degraded, whereas the GNSS signals are not. Figure 6 shows the GNSS configuration while driving through the urban canyon. Figure 7 reports the estimated location for unaided and map-aided hybridized GNSS with an emphasis on the locations where the map has been used. Additionally, Figure 8 depicts the NIS for the hybridized GNSS under the simulated urban-canyon conditions, with an emphasis on period where the map was used (yellow-area). Figure 9 presents the RMS error signal for the map-aided DR under the simulated adverse conditions.

Before entering the urban-canyon, both unaided and map-aided hybridized GNSS shows analogous results (Figure 7). This is due to the good GNSS signal condition under open-sky. Additionally, due to the availability of GNSS PR, the estimated error variance is low, leading to map rejection in several part of the path.

When driving through the urban-canyon, only 2 PR are available (Figure 6). Under these adverse conditions, the NIS estimated for both unaided and map-aided hybridized GNSS is null (Figure 8). This shows that 2 PR only are not sufficient to estimate the vehicle state. Thus, when unaided, the 2D pose (x, y, ψ) is estimated according to the WSS measurements (Figure 7). Considering the map-aided hybridized GNSS, the 2D pose estimates is enhanced as the maximum error stays under $7m$ according to Figure 9. As the estimation of the altitude and the clock-bias are linked through the PR model (Eq.5), the estimation of this value is enhanced compared to the unaided hybridized GNSS.

After the urban-canyon, open-sky conditions are retrieved. When unaided, this NIS value for the GNSS measurements increases so that the PRs are rejected (Figure 8). Thus, a significant error variance must be obtained to recover GNSS

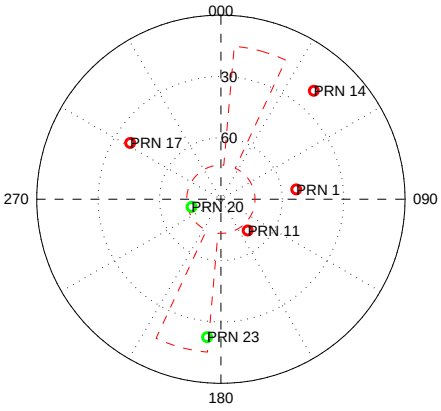

Figure 6. Skyplot for the simulated urban canyon. PRN 20 and 23 are the visible SV.

measurements. This inhere in integrity methods based on internal consistency. On the contrary, due to the correct 2D estimated location (about 4 m, Figure 9), a smaller NIS value is obtained when map-aided (Figure 8). Thus, the GNSS measurements are immediately usable. Finally, a good error variance is estimated as the map is rejected after the second roundabout (Figure 7). In this area, the map suffers from a $5m$ offset.

During the complete trail, the map measurement is used 39.5% of time. Under adverse conditions, the quality of the estimates relies on the DR when using tight integration. Using the WSS measurements for estimating angular velocity provides a noisy estimation. So, when unaided, the hybridized GNSS is not able to handle such adverse conditions. On the contrary, the map-aiding technique shows interesting benefits. On the one hand, it enhances the DR estimation process (see Sec.V-A) allowing to correct the estimated heading of the vehicle. On the other hand, adding a measurement in the fusion process increases the reliability of the system as it allows the use of fewer satellites

VI. Conclusion

In this paper, a GNSS enhancement technique has been presented. To supply a GNSS-like solution, the raw GNSS PR are tightly fused with WSS and a 2D navigable road-map. As shown, this integration can be easily done thanks to the use of a local frame. Using the DR estimates, the road selection is performed. Thanks to the selected road, a map heading observation is used. Before being fused, the GNSS PR and the map observation are both validated through an internal consistency test. This test allows the rejection of doubtful measurements. Afterward, the state estimates are updated using PR and/or map heading, if validated.

The proposed method has shown interesting results under adverse conditions and complete outage. In these situations, the map-aiding technique compensates the 2D location from odometric drift. It then allows computing a location with less than 4 available PR. Unfortunately, under severe conditions the

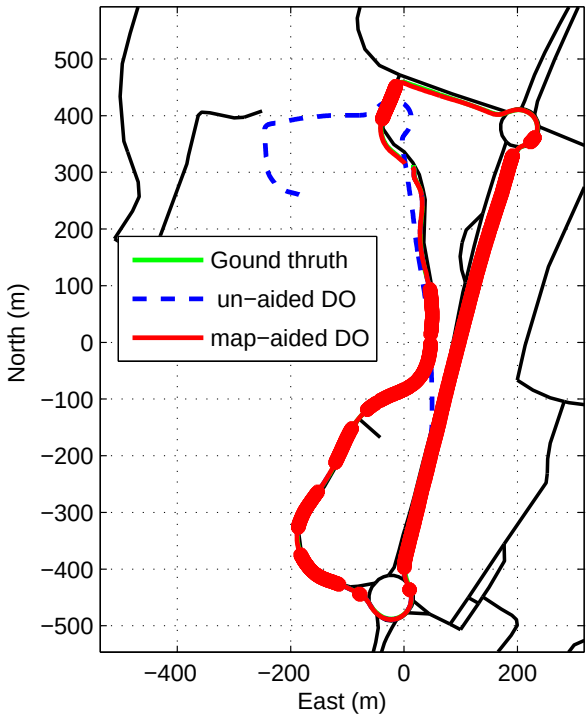

Figure 7. ENU trajectory for hybridized GNSS under simulated urban-canyon conditions.

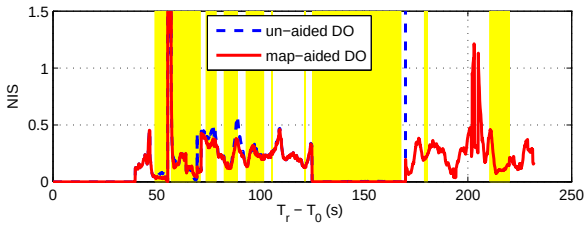

Figure 8. NIS value computed for the hybridized GNSS under simulated urban-canyon conditions.

receiver clock bias and vehicle altitude estimates are degraded. As it is difficult to provide an external information for receiver clock bias, improvements must be done regarding the altitude estimates. Therefore, the use of forthcoming 3D navigable maps is a major perspective for this research.

References

[1] E. Abbott and D. Powell, "Land-vehicle navigation using gps," *Proceedings of the IEEE*, vol. 87, no. 1, pp. 145–162, 1999.

[2] P. Bonnifait, P. Bouron, D. Meizel, and P. Crubillé, "Dynamic localization of car-like vehicles using data fusion of redundant abs sensors," *Journal of Navigation*, vol. 56, no. 3, pp. 429–441, 2003.

[3] O. Mezentsev, J. Collin, and G. Lachapelle, "Vehicular navigation in urban canyons using a high sensitivity gps receiveraugmented with a medium-grade imu," pp. 73–84, 2003.

[4] S. Sukkarieh, E. Nebot, and H. Durrant-Whyte, "A high integrity imu/gps navigation loop for autonomous land vehicle applications," *IEEE Transactions on Robotics and Automation*, vol. 15, no. 3, pp. 572–578, 1999.

[5] Y. Li, J. Wang, C. Rizos, P. Mumford, and W. Ding, "Low cost tightly coupled gps-ins integration based on a non linear kalmanfiltering design," Institute of Navigation, 2006.

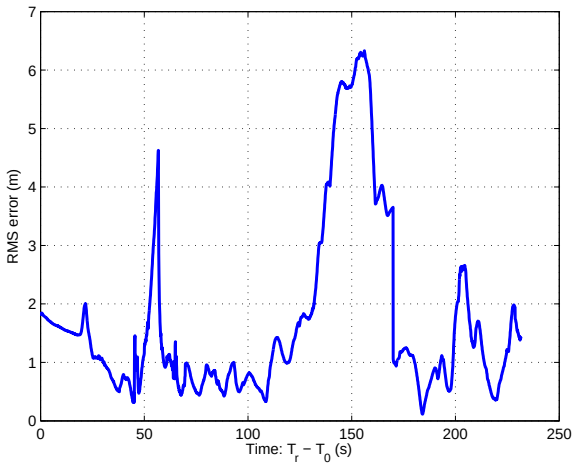

Figure 9. RMS error for map-aided DR under simulated urban-canyon conditions.

[6] T.-H. Chang, L.-S. Wang, and F.-R. Chang, "A solution to the ill-conditioned gps positioning problem in an urban environment," *Intelligent Transportation Systems, IEEE Transactions on*, vol. 10, pp. 135–145, March 2009.

[7] U. Bhatti and W. Ochieng, "Failure modes and models for integrated gps/ins systems," *Journal of Navigation*, vol. 60, no. 2, pp. 327–348, 2007.

[8] Y. Cui and S. Ge, "Autonomous vehicle positioning with gps in urban canyon environments," *IEEE Trans. on Rob. and Aut.*, vol. 19, pp. 15–25, 2003.

[9] S. Syed and M. Cannon, "Map-aided gps navigation," *GPS World*, vol. 16, no. 11, pp. 39–44, 2005.

[10] M. Quddus, W. Ochieng, and R. Noland, "Current map-matching algorithms for transport applications: State-of-the art and future research directions," *Transportation Research Part C: Emerging Technologies*, vol. 15, no. 5, pp. 312–328, 2007.

[11] C. Fouque and P. Bonnifait, "Road navigation system monitoring using a pseudorange snapshot test," in *IFAC World Congress 2008*, vol. 17, (COEX, Korea, South), 2008.

[12] A. Lahrech, C. Boucher, and J.-C. Noyer, "Accurate vehicle positioning in urban areas," *IECON Proceedings (Industrial Electronics Conference)*, vol. 5, pp. 486–490, 2005.

[13] G. Taylor and G. Blewitt, "Virtual differential gps and road reduction filtering by map matching," *Proceedings of ION99*, pp. 1675–1684, 1999.

[14] J. Li, G. Taylor, and D. Kidner, "Accuracy and reliability of map-matched gps coordinates: The dependence on terrain model resolution and interpolation algorithm," *Computers & Geosciences*, vol. 31, no. 2, pp. 241–251, 2005.

[15] D. Betaille, R. Toledo-Moreo, and J. Laneurit, "Making an enhanced map for lane location based services," in *Intelligent Transportation Systems, 2008. ITSC 2008. 11th International IEEE Conference on*, pp. 711–716, Oct. 2008.

[16] L. Kang, T. Han-Sue, and J. Hedrick, "An enhanced gps-based vehicle positioning system through sensor fusion of digital map data," in *9th International Symposium on Advanced Vehicle Control, AVEC08*, (Kobe, Japon), 6-9 octobre 2008.

[17] B. Hofmann-Wellenhof, H. Lichtenegger, and J. Collins, *GPS Theory and Practice*. Austria: Springer, fifth ed., October 1994.

[18] RTCA/DO-229C, "Minimum operational performance standards for global positioning system/wide area augmentation system airborne equipment," tech. rep., RTCA, 2001.

[19] P. Bonnifait, M. Jabbour, and G. Dherbomez, "Real-time implementation of a gis-based localization system for intelligent vehicles," *EURASIP Journal on Embedded Systems*, pp. 12–24, June 2007.

[20] A. Kelly, "Some useful results for closed-form propagation of error in vehicle odometry," tech. rep., CMU-RI-TR-00-20, 2000.

[21] M. A. Sturza and A. K. Brown, "Comparison of fixed and variable threshold raim algorithms," (NAVSYS Corp, Monument, United States), pp. 437–442, 1990.